


The N-terminal peptide of the transglutaminase-activating metalloprotease inhibitor from *Streptomyces mobaraensis* accommodates both inhibition and glutamine cross-linking sites

Norbert E. Juettner^{1,2}, Stefan Schmelz³, Anita Anderl¹, Felix Colin¹, Moritz Classen¹, Felicitas Pfeifer², Andrea Scrima³ and Hans-Lothar Fuchsbauer¹ 

¹ Department of Chemical Engineering and Biotechnology, University of Applied Sciences of Darmstadt, Germany

² Department of Biology, Technische Universität Darmstadt, Germany

³ Structural Biology of Autophagy Group, Department Structure and Function of Proteins, Helmholtz-Centre for Infection Research, Braunschweig, Germany

Keywords

crystal structure; metalloprotease inhibitor; serine protease inhibitor; *Streptomyces mobaraensis*; transglutaminase

Correspondence

H.-L. Fuchsbauer, Department of Chemical Engineering and Biotechnology, University of Applied Sciences of Darmstadt, Stephanstraße 7, Darmstadt 64295, Germany
Tel: +49 6151 1638181
E-mail: hans-lothar.fuchsbauer@h-da.de

(Received 21 March 2019, revised 1 July 2019, accepted 14 August 2019)

doi:10.1111/febs.15044

Streptomyces mobaraensis is a key player for the industrial production of the protein cross-linking enzyme microbial transglutaminase (MTG). Extra-cellular activation of MTG by the transglutaminase-activating metalloprotease (TAMP) is regulated by the TAMP inhibitory protein SSTI that belongs to the large *Streptomyces* subtilisin inhibitor (SSI) family. Despite decades of SSI research, the binding site for metalloproteases such as TAMP remained elusive in most of the SSI proteins. Moreover, SSTI is a MTG substrate, and the preferred glutamine residues for SSTI cross-linking are not determined. To address both issues, that is, determination of the TAMP and the MTG glutamine binding sites, SSTI was modified by distinct point mutations as well as elongation or truncation of the N-terminal peptide by six and three residues respectively. Structural integrity of the mutants was verified by the determination of protein melting points and supported by unimpaired subtilisin inhibitory activity. While exchange of single amino acids could not disrupt decisively the SSTI TAMP interaction, the N-terminally shortened variants clearly indicated the highly conserved Leu40-Tyr41 as binding motif for TAMP. Moreover, enzymatic biotinylation revealed that an adjacent glutamine pair, upstream from Leu40-Tyr41 in the SSTI precursor protein, is the preferred binding site of MTG. This extension peptide disturbs the interaction with TAMP. The structure of SSTI was furthermore determined by X-ray crystallography. While no structural data could be obtained for the N-terminal peptide due to flexibility, the core structure starting from Tyr41 could be determined and analysed, which superposes well with SSI-family proteins.

Enzymes

Chymotrypsin, EC 3.4.21.1; griselysin (SGMPH, SgmA), EC 3.4.24.27; snalysin (ScNP), EC 3.4.24.77; streptogrisin-A (SGPA), EC 3.4.21.80;

Abbreviations

AdpA, A-factor-dependent protein A; ArpA, A-factor receptor/repressor protein A; MTG, microbial transglutaminase; SAC, *Streptomyces* anticoagulant; SCNPI, *Streptomyces caespitosus* neutral metalloprotease inhibitor; SCNP, *Streptomyces caespitosus* neutral metalloprotease; SgiA, *Streptomyces griseus* inhibitor A; SgmA, *Streptomyces griseus* metalloprotease A (identical with SGMPH); SGMPH, *Streptomyces griseus* metalloprotease II (identical with SgmA); SGPA/SGPB, *Streptomyces griseus* (serine) protease A/B; SIL, SSI-like inhibitory protein; SSI, *Streptomyces* subtilisin inhibitor; SSTI, *Streptomyces* subtilisin and TAMP inhibitor; TAMP, transglutaminase-activating metalloprotease; TAP, tri(tetra)peptidylaminopeptidase.

streptogrisin-B (SGPB), EC 3.4.21.81; subtilisin BPN', EC 3.4.21.62; transglutaminase, EC 2.3.2.13; transglutaminase-activating metalloprotease (TAMP), EC 3.4.-.-; tri-/tetrapeptidyl aminopeptidase, EC 3.4.11.-; trypsin, EC 3.4.21.4.

Databases

The atomic coordinates and structure factors (PDB 6I0I) have been deposited in the Protein Data Bank (<http://www.rcsb.org>).

Introduction

Many actinobacteria produce small inhibitory proteins raised against serine proteases such as subtilisin BPN' (EC 3.4.21.62, UniProt code P00782), trypsin (EC 3.4.21.4, P00760), and chymotrypsin (EC 3.4.21.1, P00766). They are commonly designated as *Streptomyces* subtilisin inhibitors (SSI) or SSI-like protease inhibitors (SIL) due to the high specificity of an early and intensively studied variant from *Streptomyces albobogriseolus* S-3253 (P01006) against the alkaline serine protease, indicated by K_i in the low picomolar range [1,2]. All members of the SSI family (MEROPS I16) adopt thermoresistant protein structures consisting of two identical subunits that may undergo conformational changes from flexible to rigid structures by the attachment to the serine proteases [3]. While methionine (SSI-Met104) is responsible for strong inhibition in *S. albobogriseolus* SSI, substitution by lysine or arginine at this position allows the vast majority of streptomycetes to impair both subtilisin- and trypsin-like proteases (Fig. 1A, green box). Consequently, it has been shown that Met/Lys(Arg) and Met/Tyr(Trp) substitutions at the inhibition site of SSI conserve the subtilisin inhibitory activity but introduce new affinities for trypsin and chymotrypsin respectively [2]. Moreover, SSI proteins strongly affect activity of the *Streptomyces griseus* metalloprotease II (SGMPHII, SgmA, griselysin, B1W035/Q83WH1), which was thought to compete with subtilisin BPN' for the same inhibition site [4]. However, substitution or deletion of SSI-Met104 and adjacent amino acids could not decisively break the inhibition of SGMPHII, and dissociation constants were at most altered by one order of magnitude [5]. In contrast, the *Streptomyces caespitosus* neutral protease inhibitor (ScNPI, Q9FDS0) for the metalloprotease ScNP (snapalysin, EC 3.4.24.77, P56406), originally obtained from the undefined *Streptomyces* isolate I-355, was completely inactivated by the exchange of ScNPI-Tyr61 for alanine that is located two residues downstream from the N-terminal cysteine and opposite to the subtilisin-affine methionine

(ScNPI-Met99) [6]. It may be highly remarkable that this tyrosine is lacking, as a rule, in SSI or SIL proteins from other streptomycetes, and even in the SGMPHII inhibitory protein (Fig. 1A,B, red box).

The wide distribution of SSI and SIL has caused investigators to study the protein function in the life cycle of streptomycetes. In *S. griseus*, aerial hyphae formation and secondary metabolism is triggered by the highly conserved transcription regulator A-factor-dependent protein A (AdpA, Q9S166, B1VW60) in response to the release of the A-factor receptor/repressor protein (ArpA, Q9ZN78) [7]. Moreover, AdpA switches on a cascade of serine and metalloproteases, even comprising the *S. griseus* inhibitor A (SgiA, B1VRG2), the SSI variant from *S. griseus* [8]. While disruption of the *sgiA* gene enhances proteolytic activity without recognizable influence on aerial hyphae and spores, addition of the purified SgiA protein to surface colonies caused a delay of morphogenesis start. This result clearly underlines the relevance of SgiA in the regulation of proteases that exploit the substrate mycelium for the formation of aerial hyphae. It corresponds to the early finding that SSI inhibits, besides SGMPHII, the chymotrypsin-like *S. griseus* serine proteases A (SGPA, streptogrisin-A, EC 3.4.21.80, P00776) and B (SGPB, streptogrisin-B, EC 3.4.21.81, P00777) as strong as subtilisin BPN' [9].

We have studied activation of the protein cross-linking enzyme microbial transglutaminase (MTG, EC 2.3.2.13, P81453) by the thermolysin-like transglutaminase-activating metalloprotease (TAMP, P83543) from *Streptomyces mobaraensis* that is related to the AdpA-regulated *S. griseus* metalloprotease A (SgmA, SGMPHII) [10–12]. *S. mobaraensis* further produces the extracellular *Streptomyces* subtilisin and TAMP inhibitory protein (SSTI, P83544), likewise affecting trypsin due to lysine in place of methionine [10,11]. As is found in most SSI and SIL proteins, the ScNP-binding tyrosine of ScNPI (Tyr61) is substituted by a highly conserved proline (Pro71) in SSTI (Fig. 1B, red box). This mutation strongly disfavours ScNP-like binding

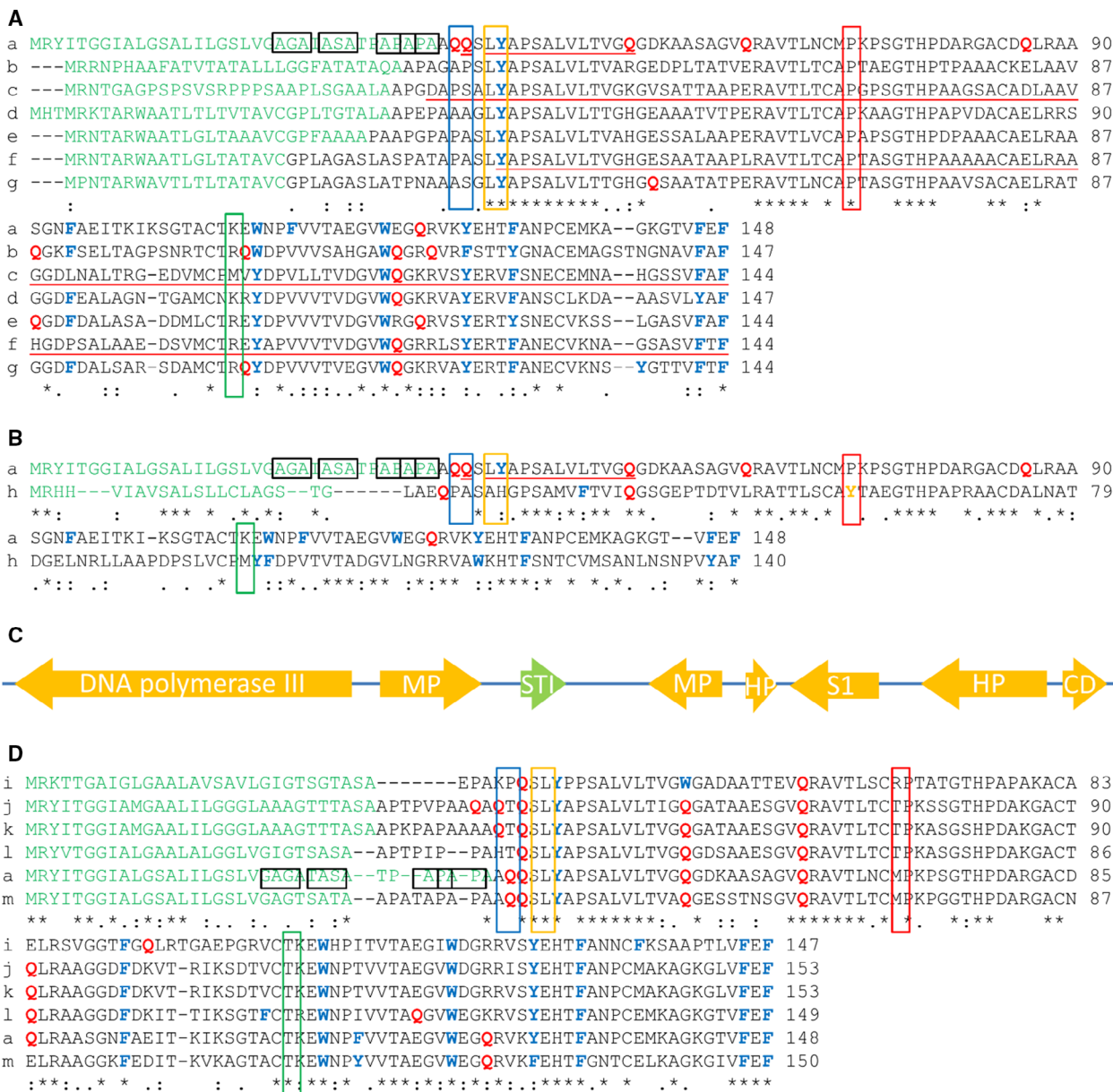


Fig. 1. Gene organization and sequence alignment of SSTI from *Streptomyces mobaraensis*. Alignment using proteins from frequently studied streptomycetes (A), the ScNP inhibitory protein ScNPI (B), and putative proteins from transglutaminase-producing streptomycetes (D) was performed by CLUSTAL OMEGA, (European Molecular Biology Laboratory, Cambridge, UK): (1) SSTI (P83544), *S. mobaraensis* (*Streptovercillium mobaraense*); (2) SgiA (B1VRG2), *Streptomyces griseus* subsp. *griseus*; (3) SSI (P01006), *Streptomyces albogriseolus*; (4) C9Z0C9, *Streptomyces scabiei*; (5) K4QWL8, *Streptomyces davaonensis*; (6) P61152, *Streptomyces coelicolor* A3(2); (7) Q825H1, *Streptomyces avermitilis*; (8) ScNPI (Q9FDS0), *Streptomyces caespitosus*; (9) A0A1S6RG02, *Streptomyces hygrosopicus*; (10) A0A2N8NML4, *Streptomyces eurocidicus*; (11) A0A1Z2L992, *Streptomyces albireticuli*; (12) A0A2G1XB55, *Streptomyces cinnamoneus* (*Sv. cinnamoneum*); (13) A0A0K9X972, *Streptomyces caatingaensis*. The putative MTG and TAMP binding sites are printed bold in red (glutamines) and blue (aromatic amino acids) colours. Black, blue, orange, red and green boxes depicted assumed binding sites of signal peptidases, MTG and TAMP as well as the determined binding sites of ScNP and the serine proteases subtilisin/trypsin. (C) Genes flanking *sstI* (green). The used abbreviations are: STI, SSTI; MP, membrane protein (incomplete); HP, hypothetical protein (M3BFW3); S1, S1 family peptidase (M3C3A5); CD, cell division protein SepF (M3AXV3).

of TAMP in the corresponding ScNPI region of SSTI. SSTI has been further shown to be provided with glutamine and lysine residues, allowing protein cross-linking by the microbial enzyme transglutaminase (MTG) [13]. Assembly with other substrate proteins and MTG-mediated cross-linking are likely to irreversibly deplete SSTI in the bacterial cell wall. Accordingly, SSTI is a putative switch regulating transglutaminase and protease activities upon onset of aerial hyphae growth in *S. mobaraensis*.

With exception of ScNPI/ScNP [6], the interaction of SSI and SSI-like proteins with metalloproteases such as SGMPII (SgmA) or TAMP remained elusive despite intensive research efforts over a period of at least three decades. Moreover, transglutaminase-producing streptomycetes such as *S. mobaraensis* (formerly *Streptovermicillium mobaraense*) have obviously evolved SSI/SIL variants such as SSTI that allows protein cross-linking via N^ε-γ-glutamyllysine isopeptide bonds. Aim of the present study was to determine the SSTI binding site for transglutaminase (glutamine donor site) and its activating metalloprotease TAMP (inhibition site). Special attention was paid to a 6–10 aa extension peptide at the SSTI N terminus exhibiting two adjacent glutamines, which are absent in SSI-like proteins from frequently studied streptomycetes (Fig. 1A, blue box). Interestingly, this double-Q-containing peptide is closely arranged to the highly conserved N-terminal peptide XLYAP that harbours hydrophobic and aromatic residues such as leucine and tyrosine (Fig. 1A, orange box), appropriate for interacting with the active core of thermolysin-like metalloproteases. Although SSTI was extensively modified via point mutations at the N-terminal peptide and the already determined binding sites for the metalloprotease ScNP and the serine proteases subtilisin/trypsin/chymotrypsin, clear results were only obtained with variants exhibiting extended or truncated SSTI N termini. We further crystallized SSTI to gain deeper insights into the MTG-accessible glutamines and the molecular structure of the TAMP-binding site, even though the N-terminal peptide of SSI is highly flexible [14]. Here, we report the protein interactions between SSTI/MTG and SSTI/TAMP as observed by kinetic and thermodynamic measurements and illuminate the respective binding sites in the structure of SSTI.

Results

Sequence information

The gene for the subtilisin and TAMP inhibitor (SSTI) is located on Contig 77 of the shotgun-sequenced genome of *S. mobaraensis* DSM 40847 [15]. Considering

ssti and *ssti*-flanking genes via BLAST-N-search (National Library of Medicine, National Center for Biotechnological Information, Bethesda, MD, USA) (Fig. 1C), we could not detect any similarities to annotated *Streptomyces* genomes. Contrary to the metalloproteases, genes encoding SSI or SIL proteins are not integrated in highly conserved gene clusters, although regulation of the *ssti* and *tamp* genes by the AdpA-like protein M3BZB1 seem to be likely [8,11]. Members of the genus *Streptomyces* have obviously acquired a precursor gene for SSI and SIL proteins in an early stage of evolution and have then modified the DNA for accomplishing various biological functions such as regulation of enzyme processing, substrate mycelium degradation or disarmament of *Bacillus subtilis*.

The SSI and SIL proteins are moderately similar, but certain features are highly conserved (Fig. 1A). Among these are four cysteines, aromatic amino acids (blue bold print), and three short segments determining the mature N terminus, as well as the first two N-terminal β-sheets and an extensive loop at the interface of each subunit (Fig. 1A). Decoration of both terminal peptides with aromatic residues may be particularly striking, even though the N-terminal Leu-Tyr motif is absent in ScNPI (Fig. 1B, orange box). In contrast, *S. mobaraensis* has evolved a subtilisin inhibitory protein (SSTI) that differs from the other SSI-like proteins by a considerable number of glutamines (Fig. 1A,D, red bold print). A glutamine pair, located upstream from Leu40-Tyr41 and only separated by a single amino acid (Ser39), appeared to us as being a special feature of SSTI from *S. mobaraensis* (Fig. 1A, blue box). Indeed, hypothetical SSTI-like proteins from transglutaminase-producing streptomycetes are likewise endowed with glutamines in similar positions (Fig. 1D).

In SSTI, the Gln-Gln and Leu-Tyr segments are separated from the starting methionine by 35 and 38 amino acids respectively (Fig. 1). The SignalP server predicted removal of the signal peptide after 33Ala-Pro-Ala35, thus suggesting short extension of the mature protein by AQQ. The presence of three additional signal peptidase motifs, Ala-Xaa-Ala, beyond this peptide, however, hardly allows estimation of the beginning of the spacer peptide (Fig. 1A,B,D, black boxes). Moreover, the proline-rich spacer sequence 29TPAPAP34 and the additional Ala42-Pro43 motif in the SSTI N terminus, downstream from Leu40-Tyr41, are appropriate binding sites for the previously characterized AP-specific tri-/tetrapeptidyl aminopeptidase (P83615) [16]. This enzyme truncates TAMP-processed transglutaminase in *S. mobaraensis* and could be involved in the regulation of proteolytic and cross-linking activities by partial hydrolysis of the putative SSTI spacer peptide [16,17].

Production of SSTI

The purified SSTI wild-type protein (*Sm*-SSTI) from *S. mobaraensis* DSM 40487 was prepared according to the published procedures [10,13]. Here, we established a procedure using *Escherichia coli* BL21 (DE3) pLysS that allows the export of *r*SSTI into the periplasm and the purification from cell supernatants by pH precipitation, Fractogel EMD SO₃⁻ and Superdex 75 chromatography (Fig. 2A,B). This process equally yielded sufficient amounts of *r*SSTI variants containing extended and shortened N termini, or distinct substitutions at the N-terminal peptide and the determined ScNP/subtilisin binding sites (Fig. 1, red/green boxes). Preparation of *r*SSTI exhibiting a 14mer spacer peptide (from Thr25 to Gln38) resulted in useless protein mixtures, due to partial truncation by *E. coli* proteases.

Determination of the TAMP inhibition site on SSTI

The exhaustive exchange of amino acids at the subtilisin-affine SSI-Met104 region (SSTI-Lys108, Fig. 1A, green box) has shown moderate effects on SSI interaction with SGMPII [4]. Moreover, the sequences of SSTI and other SSI-like inhibitory proteins largely differ from ScNPI at the Tyr61 inhibition site for the metalloprotease ScNP (Fig. 1B, red box). Nevertheless, to verify incapability of both protein segments to

attach to TAMP, we decided to replace SSTI-Lys108 (corresponding to SSI-Met104), SSTI-Glu109 (SSI-Val105), SSTI-Met70 (ScNPI-Ala60) and SSTI-Lys72 (ScNPI-Thr62) for alanine, serine, arginine and glutamate (Table 1). Additional substitutions, proposed by the SSTI protein structure, were introduced at SSTI-Ile100 and SSTI-Tyr41. Ultimately, extension and truncation of the N-terminal peptide resulted in variants containing up to six additional amino acids (aa₆-*r*SSTI) or lacking up to five amino acids (Δ SLYAP).

With exception of the SSTI variant Δ SLYAP, all heterologously produced proteins had melting points like *Sm*-SSTI, the wild-type protein from *S. mobaraensis* culture supernatants, and only differed by 0.2–3.6° or 0.3–5% (Table 1). While substitution of Lys72 for glutamate at the ScNP-preferred binding site slightly improved the intra-molecular protein interactions, removal of the N-terminal pentapeptide SLYAP, especially (Y)AP, caused considerable loss in protein stability.

The inhibitory activity of the SSTI proteins was competitively monitored by the release of yellow *para*-nitroaniline or fluorescent PheEDANS using the subtilisin substrate *Suc*AAPFpNA or the TAMP substrate *dabcy*/SFEDANS respectively [13,18]. As expected, we did not observe considerable effects on subtilisin inhibition by the point mutations chosen for SSTI (Table 1). However, the obtained IC₅₀ data, varying

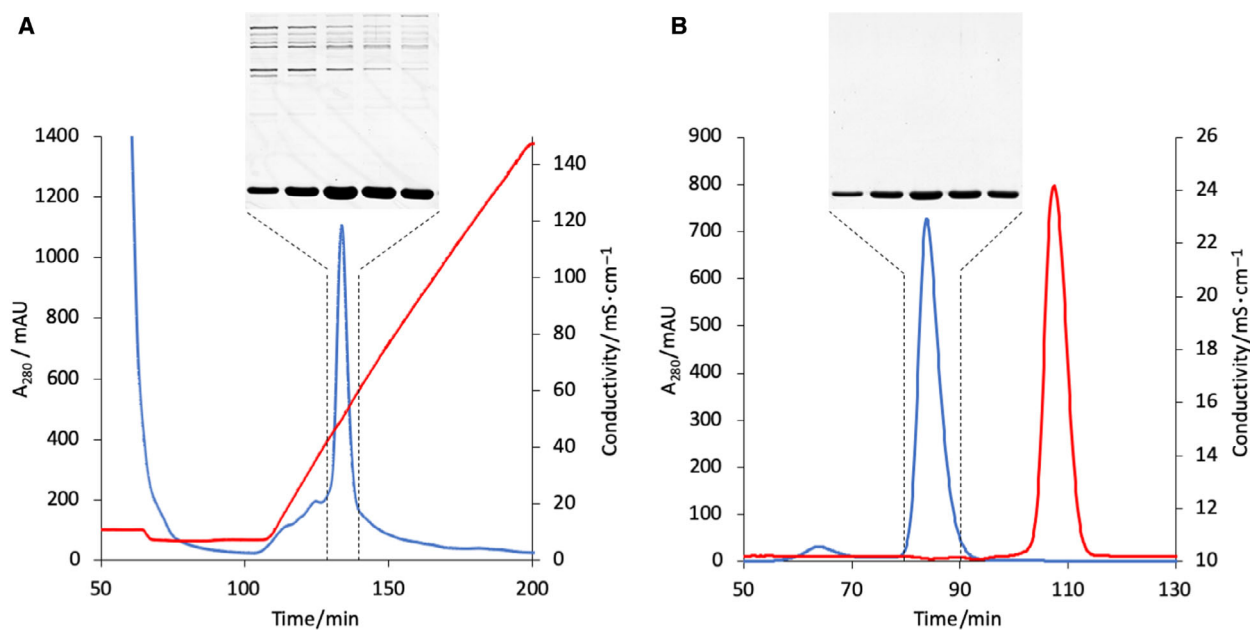


Fig. 2. Purification of *r*SSTI. (A) pH-precipitated proteins from disrupted cell supernatants were separated by Fractogel EMD SO₃⁻ chromatography (CIEX) using 0–1 M NaCl in 50 mM acetate pH 5.3. (B) Size-exclusion chromatography of combined CIEX-fractions by Superdex 75 using 100 mM NaCl in 20 mM HEPES pH 8.0. The insets depict Coomassie-stained proteins separated by 15% SDS polyacrylamide.

Table 1. Inhibition of subtilisin and TAMP by SSTI variants.

SSTI	Sequence variance	Melting point °C	Subtilisin inhibition		TAMP inhibition			
			IC ₅₀ ^a nM	IC ₅₀ ^a nM	K _d ^b nM	ΔG ^b kJ·mol ⁻¹	ΔH ^b kJ·mol ⁻¹	ΔS ^b J·(mol K) ⁻¹
<i>Sm</i> -SSTI ^c		73.1	160 ± 2.7	30.1 ± 1.7				
<i>r</i> SSTI (<i>wt</i>)	SLYAP...	72.9	159 ± 2.3	13.7 ± 0.49	< 1	-52	-75 ± 0.7	-74
K108A	...CTAEW...	72.5	97.1 ± 1.5	19.0 ± 0.68				
E109A	...CTKAW...	69.8	244 ± 3.6	13.8 ± 0.54				
K108A/E109A	...CTAAW...	69.5	134 ± 2.1	13.7 ± 0.39				
I100S	...TKSKS...	72.4	n.d.	11.7 ± 0.23				
M70S	...CSPKP...	75.4	200 ± 3.1	10.3 ± 0.25				
K72S	...CMPSP...	73.2	120 ± 2.2	14.5 ± 0.58				
K72R	...CMPRP...	72.7	216 ± 2.9	12.5 ± 0.62				
K72E	...CMPEP...	75.1	160 ± 2.9	14.1 ± 0.73				
Y41A	SLAAP...	72.2	130 ± 2.5	22.4 ± 1.4				
Y41R	SLRAP...	72.5	145 ± 2.6	33.5 ± 1.8				
aa ₆ - <i>r</i> SSTI	APAAQQS...	72.8	134 ± 2.4	108 ± 6.74	17 ± 4	-45	-51 ± 0.7	-19
aa ₃ - <i>r</i> SSTI	AQQLYA...	73.1	138 ± 2.2	63.9 ± 3.2	< 1	-52	-48 ± 0.3	+15
ΔS	SLYAP...	72.9	171 ± 2.5	15.5 ± 0.77	2.5 ± 0.8	-50	-70 ± 0.5	-65
ΔSL	SLYAP...	73.0	141 ± 2.2	2279 ± 540	401 ± 69	-37	-47 ± 1.5	-31
ΔSLY	SLYAP...	71.9	120 ± 1.8	none				
ΔSLYAP	SLYAP...	63.0	154 ± 3.4	none				

^aThe data were measured in triplicates by subtilisin- or TAMP-mediated hydrolysis of *SucAAPPpNA* or *dabcy/SFEDANS* respectively. ^bData from isothermal titration of 2 μL 100 μM SSTI aliquots (18 injections) to 200 μL 7.5 μM TAMP at 30 °C. ^cPurified from 4 days aged cultures of *Streptomyces mobaraensis*.

between 100 and 200 nM, additionally confirmed conformational integrity and functionality of all produced SSTI proteins. Furthermore, although SSTI inhibited TAMP more effectively than subtilisin, differing in one order of magnitude, the exchange of single amino acids could not decisively break mutual affinity of both proteins. The most weakened inhibitory variant, harbouring the substitution Y41R, only needed slightly enhanced concentrations to achieve *r*SSTI- or *Sm*-SSTI-like TAMP inhibition.

The extended peptides beyond the SSTI N terminus gave then rise to the assumption that TAMP might attach to that protein site. Elongation of SSTI by six amino acids reduced IC₅₀ by one order of magnitude (aa₆-*r*SSTI variant, Table 1). Even the shorter aa₃-*r*SSTI still exhibited a considerably lower inhibitory activity than SSTI-Y41R. The unexpected observation caused us to shorten the SSTI N terminus by single amino acids. Removal of the N-terminal serine (Ser39) had no influence on SSTI function (Table 1, Fig. 3A). However, additional cleavage of the adjacent leucine (Leu40) dropped SSTI activity by two orders of magnitude. Further removal of Tyr41 resulted in total loss of SSTI activity. Truncation of the following Ala-Pro

peptide had, of course, no further influence on activity. However, it should be noticed that this AP motif can be used by the tripeptidylaminopeptidase to abolish metalloprotease inhibitory activity of SSTI.

Interaction between TAMP and SSTI

The complex formation of the transglutaminase-activating metalloprotease TAMP and its inhibitory protein SSTI was further studied by size-exclusion chromatography (SEC) and isothermal titration calorimetry (ITC). While TAMP eluted from the Superdex 200 column after 1.66 mL in accordance with its molecular mass of 55 kDa, the SSTI homodimer (24 kDa) passed the detector after 1.83 mL (Fig. 3A, red/orange lines). In equimolar mixtures, absorbance of both proteins was combined in a single peak after 1.43 mL, signified by a small tailing (Fig. 3A, blue line). The determined molecular mass of this protein complex was 130 kDa and indicated that two TAMP molecules should be bound to the SSTI protein dimer. Interestingly, at SSTI excess (molar I/E ratio of 2 : 1), a second protein complex emerged after 1.61 mL (60 kDa), either consisting of TAMP and a

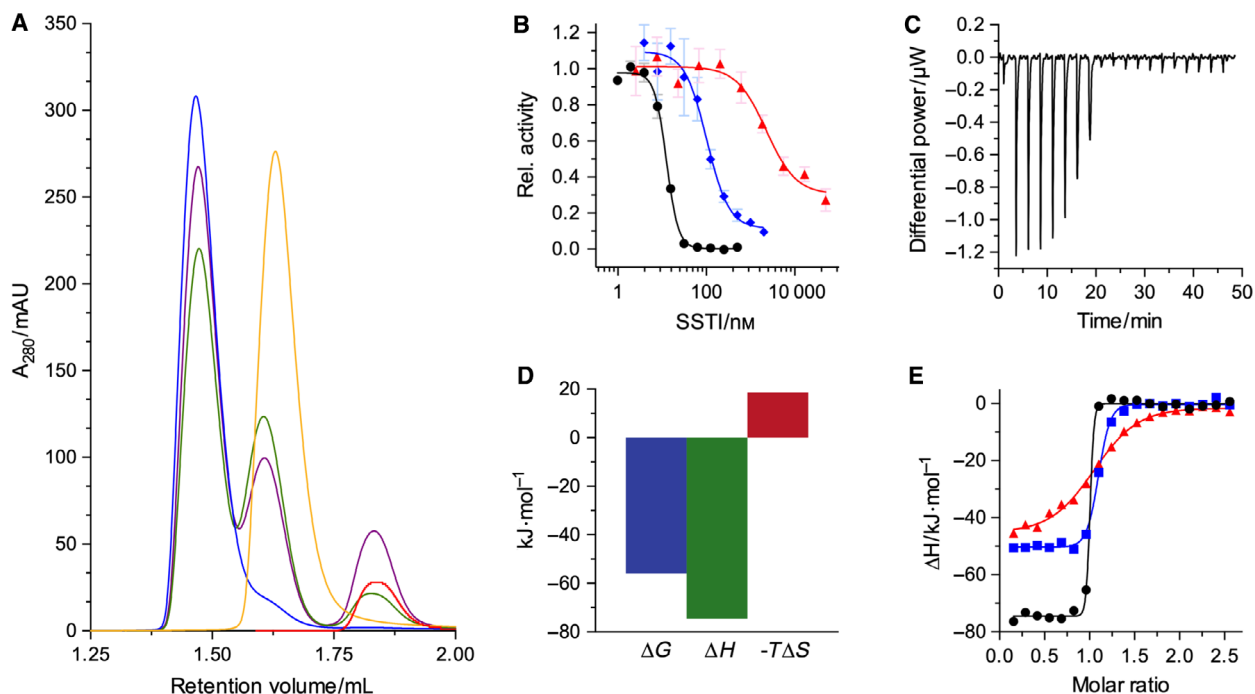


Fig. 3. Complex formation between *rSSTI* and TAMP. (A) Both proteins were incubated for 10 min at ambient temperatures and separated by Superdex 200 chromatography at pH 8.0 using a flow rate of $75 \mu\text{L}\cdot\text{min}^{-1}$: $25 \mu\text{M}$ SSTI (red); $25 \mu\text{M}$ TAMP (orange); $25 \mu\text{M}$ SSTI / $25 \mu\text{M}$ TAMP (blue); $50 \mu\text{M}$ SSTI / $25 \mu\text{M}$ TAMP (green); $75 \mu\text{M}$ SSTI / $25 \mu\text{M}$ TAMP (purple). (B) Effect of SSTI on TAMP activity. Residual activity was determined using 5 nM TAMP, $0.05\text{--}50 \mu\text{M}$ SSTI and $2 \mu\text{M}$ *dabcyl*/SFEDANS in 100 mM Tris/acetate and 2 mM CaCl_2 pH 8.0 (final volume of $200 \mu\text{L}$) at $30 \text{ }^\circ\text{C}$ for 10 min by increase in fluorescence at 520 nm (λ_{exc} of 340 nm). The data were obtained by three independent measurements. Error bars are depicted. (C–E) The isothermal titration calorimetry was performed by $2 \mu\text{L}$ injections of $100 \mu\text{M}$ *rSSTI* in 20 mM HEPES and 100 mM NaCl pH 6.0– $10 \mu\text{M}$ TAMP. The raw data (C) were evaluated by the internal software (D, E): aa₆-SSTI (red line with red triangles); *rSSTI* (blue line with blue squares); ΔSL (black line with black circles).

single subunit or TAMP and the dimeric inhibitory protein (Fig. 3A, green line). Further increase in the SSTI concentration (*I/E* ratio of 3 : 1) had no additional effect (Fig. 3B, purple line).

Activity and ITC measurements were in line with $\text{SSTI}_2\text{TAMP}_2$ complex formation as observed by SEC (Fig. 3B–E). Attraction of both proteins was an enthalpy-driven process, and the dissociation constant K_d was below the ITC detection limit (Table 1, Fig. 3C–E). The ITC study further revealed excellent correlation with the kinetic data of TAMP inhibition by the extended and shortened SSTI variants. The increased K_d of the $6\text{aa-}r\text{SSTI}$ and ΔSL variants corresponded well with the lower inhibitory activity, and the $\Delta\text{SLY}/\Delta\text{SLYAP}$ proteins failed to interact with TAMP (not shown). Noticeably, the complex formation of $3\text{aa-}r\text{SSTI}$ (+AQQ) and $6\text{aa-}r\text{SSTI}$ (+APAAQQ) with TAMP yielded in a positive or, at least, considerably less negative entropy as compared to the wild-type or the N-terminally shortened proteins. We assume that the hydrophobic extension peptide is highly flexible and incapable of interacting with

the core protein of SSTI [14]. The observed increase in entropy may then result from an energy-rich interface between water and the hydrophobic peptide that is abolished by the attachment of TAMP.

Determination of the SSTI glutamine donor site for transglutaminase

Former NMR studies have shown flexibility of the N-terminal peptide of SSI from *S. albobrivoles* [14]. Despite a low similarity, the extension peptide of SSTI from *S. mobaraensis*, upstream from the LY motif, shares at least four amino acids with the SSI N terminus (*cf.* Fig. 1A). Flexibility of the SSTI extension peptide was further suggested by the ITC measurements in this report. Contrary to SSI and many SIL proteins, SSTI contains two adjacent glutamine residues that represent the most probable glutamine donor sites for cross-linking by transglutaminase (MTG). Both residues, located in the SSTI extension peptide, obviously exhibit the required degrees of freedom to enter the MTG active core [19–21].

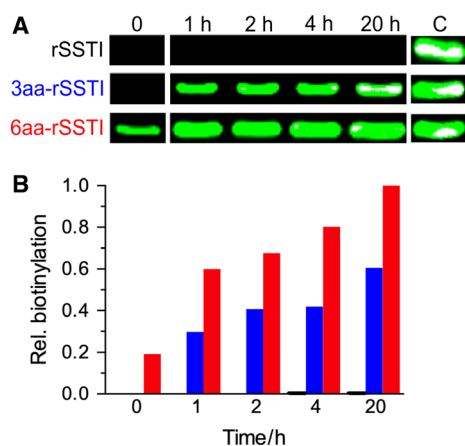


Fig. 4. Biotinylation of SSTI by transglutaminase. Labelling was carried out by incubation of $7.5 \mu\text{M}$ SSTI, $100 \mu\text{M}$ biotin cadaverine, and 75 nM MTG in 20 mM Tris/ 100 mM NaCl pH 8.0 at 37°C for the indicated times. The mixtures were separated by SDS/PAGE, blotted and visualized by streptavidin IRDye 800 CW conjugates. (A) Protein blots. (B) Relative biotinylation as obtained by evaluation of fluorescence intensity of normalized protein band areas. 6aa-rSSTI after incubation for 20 h was used as control.

Glutamine accessibility of MTG was determined by enzymatic conjugation of SSTI with biotin cadaverine (5-biotinylamidopentylamine) as previously described [19,20]. The biotinylated proteins were separated by electrophoresis, blotted and visualized by fluorescent streptavidin IRDye 800 CW conjugates. This enzymatic biotinylation assay was a qualitative experiment, and only scanning of equal protein band areas allows the semi-quantitative determination of biotin incorporation rates (Fig. 4). Nevertheless, we obtained clear results from single measurements by simultaneous labelling of the three variants and investigation of several aliquots drawn at various times.

Applying this method, biotinylation of rSSTI by MTG failed under the conditions used, thus indicate that the four glutamines of the protein core are not accessible for the enzyme. The result was in accordance with our former observation that SSTI loses the reactive glutamines during the culturing of *S. mobaraensis* [13,17]. However, if the SSTI variants AQQ-SSTI (aa₃-SSTI) and APAAQQ-SSTI (aa₆-SSTI) were incubated with biotin cadaverine and MTG, protein labelling occurred as suggested by strong fluorescent bands. Interestingly, the biotinylation rate of the most extended variant, aa₆-rSSTI, was considerably faster than that of the shorter aa₃-rSSTI. TAMP inhibitory activity and glutamine accessibility for MTG are obviously counter-regulated functions of SSTI and raise

the question of how a more extended variant may influence SSTI. The result confirmed that MTG-reactive glutamines are preferably located in flexible protein regions, especially at the terminal ends [20,21]. MTG-mediated side-chain hydrolysis, however, is most likely not the reason for loss of reactive glutamines in the course of *S. mobaraensis* growth as hypothesized earlier [13], but successive removal of the N-terminal extension peptide.

Crystal structure of SSTI

Crystals, grown from *Sm*-SSTI, belong to the $P2_1$ space group and diffracted to 1.45 \AA resolution with synchrotron radiation. The monomeric structure includes 108 residues (Y41-F148) and is composed of a four-stranded antiparallel β -sheet and three α -helices with two disulfide bridges between Cys69-84 and Cys106-136 respectively (Fig. 5A). The asymmetric unit holds a SSTI dimer, formed by the antiparallel β -sheet of each monomer generating a noncrystallographic twofold symmetry axis. Based on the PDBE-PISA server, this dimer has a buried area of 1720 \AA^2 and is stable in solution, consistent with the SEC data.

The overall structure of SSTI superposes well with other published structures of subtilisin inhibitors (e.g. SSI) with an RMSD of less than 1 \AA . Interestingly, the subtilisin binding loop (K99-P112 for SSTI) is misaligned in comparison to those of SSI structures. However, superposition based on the subtilisin binding loop itself shows that the P1 residue Lys108 is aligning with P1 residue Met104 of SSI, when bound to subtilisin (Fig. 5B,C), suggesting a slight rearrangement of the loop upon interaction. The observed tilt of the binding loop is most likely caused by SSTI crystal packing, since residues of an adjacent protein entity in the crystal would otherwise clash.

Structural data for SSTI also allow for a detailed analysis of the accessibility of the putative glutamine donor sites for MTG in the SSTI-core structure. Of the four glutamine residues in the core of the SSTI-monomer, Gln86 is buried, while Gln52, Gln62 and Gln124 are solvent exposed. However, Gln52 and Gln62 are on the flat surface of the central β -sheet and are thus less likely to be accommodated in the MTG cleft. And under the assumption that SSTI is present as dimer in solution, the accessibility of Gln86 is restricted by dimerization of SSTI. Overall, in line with the biochemical data, the four (eight in the dimer) potential glutamine donor sites in the SSTI dimer are unlikely to act as MTG-substrates due to low accessibility. In contrast, the glutamine pair is in the

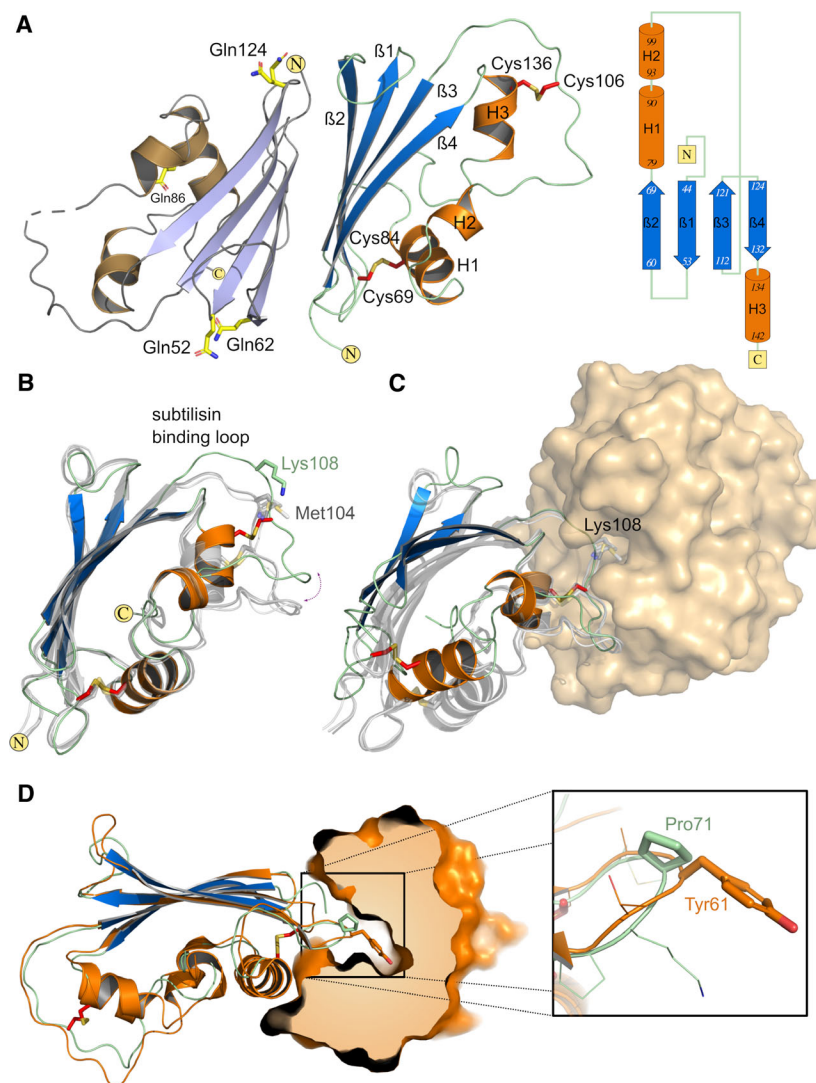


Fig. 5. Structural data of SSSI. (A) SSSI homodimer in cartoon mode. Secondary structure elements of SSSI are shown in the same colour as in the depicted topology diagram (left hand side). The four glutamines in the core structure are shown as stick representation on the monomer on the left. (B) Structure comparison of SSSI (coloured as in A) with SSI from *Streptomyces albogriseolus* (PDB 2SIC, 3SIC, 3SSI, 5SIC, coloured in grey). Superposition based on all residues indicates that the subtilisin binding loop of SSSI including the P1 residue Lys108 is shifted in reference to SSI and its P1 residue Met104. (C) Superposition based on the subtilisin binding loops (aa 99–112 for SSSI) shows no major difference in the P1 residue orientation. Subtilisin is illustrated in surface mode (coloured in sand). (D) Superposition of SSSI (coloured as in A) with the ScNP-binding turn of ScNP inhibitor structure (PDB 4HX3, coloured in orange). The surface of *Streptomyces caespitosus* snapalysin (ScNP) is shown in orange, clipped to the S1 pocket. P1 Tyr61 of ScNPI (orange) bound to ScNP reaches into the S1 pocket (close up panel, without ScNPI surface). SSSI adopts a similar binding turn structure, but Pro71 is not able to reach into the S1 pocket of ScNP.

unstructured extension peptide, which likely allows for unrestricted access for MTG explaining the rapid incorporation of biotin cadaverine into APAAQ-SSTI (aa₆-SSTI).

As mentioned above, the ScNP-binding tyrosine of ScNPI (Tyr61) is substituted by a highly conserved proline (Pro71) in SSSI. In the structure alignment of SSSI with *S. caespitosus* snapalysin (ScNP) inhibitor (PDB 4HX3) [22], the overall structure of the binding turn superposes well with an RMSD of 1 Å. Despite the similar backbone conformation, the structure gives rise to the notion that Pro71 of SSSI is likely to weaken or hinder binding into the S1' position of ScNP, as it lacks the aromatic side chain and hydroxyl group of Tyr61 of ScNPI, which is accommodated deep in the protease S1' pocket of the ScNP-ScNPI-complex.

Discussion

In streptomycetes, the formation of aerial mycelium and spores requires a plethora of enzymes such as nucleases, glycosidases and proteases that exploit the polymeric substances, stored in the vegetative hyphae [8,23]. Protein degradation is performed by a series of serine and metalloproteases, which may be regulated by multi-functional protease inhibitory proteins, denominated as *Streptomyces* subtilisin inhibitors (SSI, SIL). The high specificity for the name-giving *Bacillus* subtilisins gives rise to the assumption that SSI/SIL proteins are even used in the defense against nutrient competitors and predators.

Due to the omnipresence in streptomycetes, SSI proteins were early discovered and intensively studied for more than three decades up to the late nineties

(for an overview see ref. [24]). The authors especially focused on the frequently described inhibition site for serine proteases, an extended loop opposite to the interface between both identical subunits and detained by the C-terminal α -helix cysteine bridge. In SSI from *S. albogriseolus* S-3253, the primary inhibition site is a methionine (SSI Met104, Fig. 1A) that occupies the S1 pocket of subtilisin BPN' in the binary crystal [3,25]. Replacement of this methionine by lysine and arginine allows SSI variants from other streptomycetes, among them SSTI from *S. mobaraensis*, for strong inhibition of trypsin-like endopeptidases as well (*cf.* Fig. 1A,C). SSI and SSI-related proteins have been also shown to inhibit metalloproteases [4,6,10]. Active site and mode of action subdivide them into two types of metalloprotease inhibitors, either ScNPI-like or more abundant SSI-like variants primed with tyrosine (ScNPI-Tyr61, Fig. 1B) or proline (SSI-Pro68, Fig. 1A) in the β 2/ β 3-connecting turn, respectively, two residues downstream from the N-terminal cysteine bridge. In this study, we have shown that SSTI belongs to the SSI-related metalloprotease inhibitors, although the proposed SGMPH inhibition site for the transglutaminase-activating metalloprotease TAMP could not be confirmed [5]. Activity of TAMP was clearly affected by the N-terminal SSTI peptide, accommodating the highly conserved sequence motif Leu40-Tyr41 (Fig. 1A,D). The removal of both amino acids resulted in full depletion of inhibitory activity. We assume that SSI and other SSI-like metalloprotease inhibitors such as SgiA use, alike SSTI, this inhibition site, despite the fact that the exchange of amino acids within the subtilisin binding loop may alter the dissociation constant by one order of magnitude [5]. Our conclusion was supported by former studies with SSI-like *Streptomyces cinnamoneus* subsp. *cinnamoneus* anticoagulants (SAC, Q7M1B5) exhibiting N termini shortened by Ser-Leu-(SAC II) and Ser-Leu-Tyr-(SAC III) [26]. Both truncated proteins had lost inhibitory activity for the metalloprotease thermolysin but not for subtilisin. Moreover, although solvent accessibility has been assigned to all SSI tyrosines, and, in the crystal structure, SSI-Tyr106 (SSTI-Tyr110) seemed to be more exposed than SSI-Tyr38 (SSTI-Tyr41) [27–30], solvation of SSI-Tyr106 was dependent on increasing temperatures, and SSI-Tyr38 was more easily modified by tetranitromethane [29,30]. A $^1\text{H-NMR}$ study noted in addition that the N-terminal peptide of SSI is free and undergoes rapid motions on the nanosecond timescale [14]. Such flexibility explains why we and others could not determine the structure of the N terminus and even not of the fused SSTI extension peptide.

The ITC measurements, performed by this study, indirectly confirmed that the SSTI extension peptide is most likely surrounded by water, thereby forming energy-rich interfaces. Elimination of the highly ordered water structures may be the probable reason why complex formation between AQQ-SSTI (aa₃-SSTI) and TAMP increased the entropy in contrast to unmodified rSSTI and shortened variants. Moreover, rapid incorporation of biotin cadaverine into APAAQQ-SSTI (aa₆-SSTI) impressively displayed unrestricted access of microbial transglutaminase (MTG) to the extension peptide and, thus, to the glutamine pair. Protein labelling immediately occurred upon addition of the enzyme and was nearly completed within 30 min. Interestingly, in aa₆-SSTI the inhibitory activity for TAMP is considerably reduced, thus showing that interaction of MTG and TAMP with SSTI is counter-regulated by the extension peptide. Moreover, truncation of SSTI and loss of MTG-accessible glutamines can be readily observed during culture of *S. mobaraensis* [13,17]. The abundance of AP motifs in the extension peptide suggests the successive cleavage by the tripeptidyl aminopeptidase (TAP), produced in an early stage of culture [16].

Conclusions

The so-called *Streptomyces* subtilisin inhibitors (SSI, SIL) are proteins that regulate proteolytic activity of both serine and metalloproteases in the bacterial cell wall of aerial hyphae and spores. If genes for transglutaminase (MTG) are available, cross-linking of SSI/SIL proteins may occur in addition. We have shown that the inhibition site for the transglutaminase-activating metalloprotease (TAMP), a highly conserved Leu-Tyr motif, is found at the N terminus of the inhibitory protein SSTI, next to the glutamine donor site for MTG at a fused extension peptide. Our results do not only suggest that the majority of SSI proteins inhibit metalloproteases. They are most likely regulated by a tripeptidyl aminopeptidase via successive truncation of the N-terminal SSTI peptide. In the case of MTG-producing *S. mobaraensis*, removal of the SSTI glutamine pair interrupts SSTI cross-linking. As a consequence, recovery of full SSTI inhibitory activity prevents TAMP-mediated MTG activation.

Experimental procedures

Published procedures

Methods for the production of the transglutaminase-activating metalloprotease (TAMP) in *E. coli* [11], the

Table 2. Data collection and refinement statistics. Statistics for the highest resolution shell are shown in parentheses.

	SSTI
Data collection	
Wavelength	0.918409
Space group	$P2_1$
a, b, c (Å)	46.5, 35.2, 64.0
α, β, γ (°)	90, 105.7, 90
Resolution (Å)	44.75–1.45 (1.47–1.45)
R_{merge} (%)	0.100 (0.909)
R_{pim} (%)	0.070 (0.744)
$CC_{1/2}$	0.996 (0.414)
No. reflections	35535 (1593)
Average I/σ	8.3 (1.1)
Completeness (%)	99.3 (90.9)
Redundancy	3.7(2.9)
Wilson B-factor (Å ²)	10.4
Refinement	
Resolution (Å)	44.75–1.45
R work/ R free (%)	0.194/0.229
No. of monomers in ASU	2
No. atoms	1996
Average isotropic $B_{\text{(protein)}}$ (Å ²)	16.2
Average isotropic $B_{\text{(solvent)}}$ (Å ²)	28.2
r.m.s.d. Bond lengths (Å)	0.005
r.m.s.d. Bond angles (°)	0.774
Ramachandran plot (%)	
Favoured	98.6
Allowed	1.4
Outlier	0.0
Outliers (%)	
Rotamer	0
Bond/Angles	0/0
Chirality/Planarity	0/0
Clashscore	3.84
Molprobability score	1.17

production of microbial transglutaminase (MTG) and SSTI by culturing *S. mobaraensis* [10,13,31], the measurement of subtilisin and TAMP activity using *SucA*PFpNA and *dabcy/SFEDANS* [13,18], melting points [20], protein complex formation by analytical Superdex 200 chromatography [32], thermodynamic data by isothermal titration calorimetry [11], the MTG-mediated biotinylation [19,20] as well as general procedures such as protein content analysis, SDS/PAGE, protein blotting *etc.* are described in the indicated literature.

Production of recombinant SSTI in *E. coli*

A synthesized gene for SSTI (GenScript, Piscataway, NJ, USA) in pET22b(+) was used to transform *E. coli* BL21 (DE3)pLysS. Growth was allowed in 1 L LB medium (10 g·L⁻¹ glucose, 5 g·L⁻¹ yeast extract, 10 g·L⁻¹ NaCl) under shaking (125 r.p.m.) at 37 °C up to OD₆₀₀ of 0.4–0.6

prior to the induction with 1 mM IPTG. Upon continued culture at 28 °C for 5 h, cell lysis by sonication and spinning (20 000 g, 4 °C, 20 min), most of the *E. coli* proteins were precipitated by reducing the pH to 5.3. The remaining proteins were separated by Fractogel EMD SO₃⁻ chromatography (bed volume of 30 mL) at pH 5.3 and 2 mL·min⁻¹ using 50 mM acetate and linear increasing NaCl of 0–1 M. Final purification of the combined and concentrated SSTI fractions in 20 mM HEPES/100 mM NaCl was performed at pH 8.0 and flow rates of 1 mL·min⁻¹ by Superdex 75 chromatography (bed volume of 120 mL). The SSTI variants were prepared by amino acid substitution via SOE-PCR and purified by the described procedure.

Determination of SSTI structure

Sm-SSTI, purified from supernatants of *S. mobaraensis* cultures, was crystallized using the sitting-drop vapour diffusion method by mixing equal volumes of 14 mg·mL⁻¹ protein and precipitant solution. Plate-like crystals grew within 14 days to full size (280 × 50 × 10 μm) in 1.3 M sodium citrate, 50 mM HEPES pH 7.5 at 20 °C. Crystals diffracted to 1.45 Å in $P2_1$ space group. Diffraction data were collected on BL14.1 beamline at BESSY II (HZB, Berlin, Germany). Data were processed and scaled using XDS [33] and AIMLESS [34] respectively. The structure of *Streptomyces* subtilisin inhibitor (PDB 2SIC) was used as an initial search model for molecular replacement with PHASER [35]. The final model was built manually using COOT [36] with iterative refinement steps of PHENIX.REFINE (PHENIX package [37]). Data and refinement statistics are summarized in Table 2. Structure data has been analysed with PDBEPIA [38] and was deposited in the Protein Data Bank (PDB) with the ID 610I.

Acknowledgements

NEJ was supported by a grant of the graduate school of the University of Applied Sciences of Darmstadt. Work in the group of AS was partially funded by the Helmholtz Association Young Investigator grant number VH-NG-727. Diffraction data have been collected on BL14.1 at the BESSY II electron storage ring operated by the Helmholtz-Zentrum Berlin [39]. We are grateful to the staff for assistance during the experiment. Open access funding enabled and organized by Projekt DEAL.

[Correction added on 13 November 2020, after first online publication: Projekt Deal funding statement has been added.]

Conflict of interest

The authors declare no conflict of interest.

Author contributions

NEJ, SS, AS and HLF designed the research and wrote the paper with comments from FP; NEJ, SS, AA, MC and FC performed the research; NEJ, SS, FP, AS and HLF analysed the data.

References

- Ikenaka T, Odani S, Sakai M, Nabeshima Y, Sato S & Murao S (1974) Amino acid sequence of an alkaline protease inhibitor (*Streptomyces* subtilisin inhibitor) from *Streptomyces albogriseolus* S-3253. *J Biochem* **76**, 1191–1209.
- Koshima S, Nishiyama Y, Kumagai I & Miura K (1991) Inhibition of subtilisin BPN' by reaction site P1 mutants of *Streptomyces* subtilisin inhibitor. *J Biochem* **109**, 377–382.
- Mitsui Y, Satow Y, Watanabe Y, Hirono S & Iitaka Y (1979) Crystal structures of *Streptomyces* subtilisin inhibitor and its complex with subtilisin BPN'. *Nature* **277**, 447–452.
- Kumazaki T, Kashiwara K, Kojima S, Miura KI & Ishii SI (1993) Interaction of *Streptomyces* subtilisin inhibitor (SSI) with *Streptomyces griseus* metallo-endopeptidase II (SGMP II). *J Biochem* **114**, 570–575.
- Kashiwara K, Fujita A, Tsuyuki H, Kumazaki T & Ishii SI (1991) Interactions of *Streptomyces* serine-protease inhibitors with *Streptomyces griseus* metalloendopeptidase II. *J Biochem* **110**, 350–354.
- Hiraga K, Suzuki T & Oda K (2000) A novel double-headed proteinaceous inhibitor of metalloproteinase and serine proteinase. *J Biol Chem* **275**, 25173–25179.
- Ohnishi Y, Yamazaki H, Kato JY, Tomono A & Horinouchi S (2005) AdpA, a central transcriptional regulator in the A-factor regulatory cascade that leads to morphological development and secondary metabolism in *Streptomyces griseus*. *Biosci Biotechnol Biochem* **69**, 431–439.
- Hirano S, Kato JY, Ohnishi Y & Horinouchi S (2006) Control of the *Streptomyces* subtilisin inhibitor gene by AdpA in the A-factor regulatory cascade of *Streptomyces griseus*. *J Bacteriol* **188**, 6207–6216.
- Christensen U, Ishida S, Ishii SI, Mitsui Y, Iitaka Y, McClarin J & Langridge R (1985) Interactions of *Streptomyces* subtilisin inhibitor with *Streptomyces griseus* proteases A and B. Enzyme kinetic and computer simulation studies. *J Biochem* **98**, 1263–1274.
- Zotzel J, Keller P & Fuchsbauer HL (2003) Transglutaminase from *Streptomyces mobaraensis* is activated by an endogenous metalloprotease. *Eur J Biochem* **270**, 3214–3222.
- Juettner NE, Classen M, Colin F, Hoffmann SB, Meyners C, Pfeifer F & Fuchsbauer HL (2018) Features of the transglutaminase-activating metalloprotease from *Streptomyces mobaraensis* DSM 40847 produced in *Escherichia coli*. *J Biotechnol* **281**, 115–122.
- Kato JY, Suzuki A, Yamazaki H, Ohnishi Y & Horinouchi S (2002) Control by A-factor of a metalloprotease gene involved in aerial mycelium formation in *Streptomyces griseus*. *J Bacteriol* **184**, 6016–6025.
- Schmidt S, Adolf F & Fuchsbauer HL (2008) The transglutaminase activating metalloprotease inhibitor from *Streptomyces mobaraensis* is a glutamine and a lysine donor substrate of the intrinsic transglutaminase. *FEBS Lett* **582**, 3132–3138.
- Akasaka K (1985) ¹H n.m.r. spektrum from the flexible N-terminal segment of *Streptomyces* subtilisin inhibitor. *Int J Pept Protein Res* **25**, 547–553.
- Yang H, He T, Wu W, Zhu W, Lu B & Sun W (2013) Whole-genome shotgun assembly and analysis of the genome of *Streptomyces mobaraensis* DSM 40847, a strain for industrial production of microbial transglutaminase. *Genome Announc* **1**, e0014313.
- Zotzel J, Pasternack R, Pelzer C, Ziegert D, Mainusch M & Fuchsbauer HL (2003) Activated transglutaminase from *Streptomyces mobaraensis* is processed by a tripeptidyl aminopeptidase in the final step. *Eur J Biochem* **270**, 4149–4155.
- Zindel S, Ehret V, Ehret M, Hentschel M, Witt S, Krämer A, Fiebig D, Juettner N, Froels S, Pfeifer F *et al.* (2016) Involvement of a novel class C beta-lactamase in the transglutaminase mediated cross-linking cascade of *Streptomyces mobaraensis* DSM 40847. *PLoS One* **11**, e0149145.
- Weimer S, Oertel K & Fuchsbauer HL (2006) A quenched fluorescent dipeptide for assaying dispase- and thermolysin-like proteases. *Anal Biochem* **352**, 110–119.
- Fiebig D, Schmelz S, Zindel S, Ehret V, Beck J, Ebenig A, Ehret M, Fröls S, Pfeifer F, Kolmar H *et al.* (2016) Structure of the Dispase autolysis-inducing protein and glutamine cross-linking sites for transglutaminase. *J Biol Chem* **291**, 20417–20426.
- Juettner NE, Schmelz S, Bogen JP, Happel D, Fessner WD, Pfeifer F, Fuchsbauer HL & Scrima A (2018) Illuminating structure and acyl donor sites of a physiological transglutaminase substrate from *Streptomyces mobaraensis*. *Protein Sci* **27**, 910–922.
- Juettner NE, Schmelz S, Krämer A, Knapp S, Becker B, Kolmar H, Scrima A & Fuchsbauer HL (2018) Structure of a glutamine mimicking inhibitory protein shaped by the catalytic cleft of microbial transglutaminase. *FEBS J* **285**, 4684–4694.
- Trillo-Muyo S, Martinez-Rodriguez S, Arolas JL & Gomis-Ruth FX (2013) Mechanism of action of a Janus-faced single-domain protein inhibitor simultaneously targeting two peptidase classes. *Chem Sci* **4**, 791–797.

- 23 Nicieza RG, Huergo J, Conolly BA & Sanchez J (1999) Purification, characterization, and role of nucleases and serine proteases in *Streptomyces* differentiation. Analogies with the biochemical processes described in late steps of eukaryotic apoptosis. *J Biol Chem* **274**, 20366–20375.
- 24 Terabe M, Kojima S, Taguchi S, Momose H & Miura KI (1996) New subtilisin-trypsin inhibitors produced by *Streptomyces*: primary structures and their relationship to other proteinase inhibitors from *Streptomyces*. *Biochim Biophys Acta* **1292**, 233–240.
- 25 Takeuchi Y, Satow Y, Nakamura KT & Mitsui Y (1991) Refined crystal structure of the complex of subtilisin BPN' and *Streptomyces* subtilisin inhibitor at 1.8 Å resolution. *J Mol Biol* **221**, 309–325.
- 26 Tanabe M, Asano T, Moriya N, Sugino H & Kakinuma A (1994) Isolation and characterization of *Streptovercillium* anticoagulant (SAC), a novel protein inhibitor of blood coagulation produced by *Streptovercillium cinnamoneum* subsp. *cinnamoneum*. *J Biochem* **115**, 743–751.
- 27 Inouye K, Tonomura B, Hiromi K, Sato S & Murao S (1977) The states of tyrosyl and tryptophyl residues in a protein proteinase inhibitor (*Streptomyces* subtilisin inhibitor). *J Biochem* **82**, 1207–1215.
- 28 Satow J, Watanabe Y & Mitsui Y (1980) Solvent accessibility and microenvironment in a bacterial protein proteinase inhibitor SSI (*Streptomyces* subtilisin inhibitor). *J Biochem* **88**, 1739–1755.
- 29 Fujii S, Akasaka K & Hatano H (1981) Proton magnetic resonance study of *Streptomyces* subtilisin inhibitor. pH titration and assignments of individual tyrosyl resonances. *Biochemistry* **20**, 518–523.
- 30 Akasaka K, Fujii S & Kaptein R (1981) Exposure of aromatic residues of *Streptomyces* subtilisin inhibitor. A photo-CIDNP study. *J Biochem* **89**, 1945–1949.
- 31 Gerber U, Jucknischke U, Putzien S & Fuchsbauer HL (1994) A rapid and simple method for the purification of transglutaminase from *Streptovercillium mobaraense*. *Biochem J* **299**, 825–829.
- 32 Fiebig D, Storka J, Roeder M, Meyners C, Schmelz S, Blankenfeldt W, Scrima A, Kolmar H & Fuchsbauer HL (2018) Destructive twisting of neutral metalloproteases: the catalysis mechanism of the Dispaase autolysis inducing protein from *Streptomyces mobaraensis* DSM 40487. *FEBS J* **285**, 4246–4264.
- 33 Kabsch W (2010) Xds. *Acta Crystallogr D* **66**, 125–132.
- 34 Winn MD, Ballard CC, Kowtan KD, Dodson EJ, Emsley P, Evans PR, Keegan RM, Krissinel EB, Leslie AG, McCoy A *et al.* (2011) Overview of the CCP4 suite and current developments. *Acta Crystallogr D* **67**, 235–242.
- 35 McCoy AJ, Grosse-Kunstleve RW, Adams PD, Winn MD, Storoni LC & Read RJ (2007) Phaser crystallographic software. *J Appl Crystallogr* **40**, 658–674.
- 36 Emsley P, Lohkamp B, Scott WG & Cowtan K (2010) Features and development of Coot. *Acta Crystallogr D* **66**, 486–501.
- 37 Afonine PV, Grosse-Kunstleve RW, Echols N, Headd JJ, Moriarty NW, Mustyakimov M, Terwilliger TC, Urzhumtsev A, Zwart PH & Adams PD (2012) Towards automated crystallographic structure refinement with phenix.refine. *Acta Crystallogr D* **68**, 352–367.
- 38 Krissinel E & Henrick K (2007) Inference of macromolecular assemblies from crystalline state. *J Mol Biol* **372**, 774–797.
- 39 Mueller U, Förster R, Hellmig M, Huschmann FU, Kastner A, Malecki P, Pühringer S, Röwer M, Sparta K, Steffien M *et al.* (2015) The macromolecular crystallography beamlines at BESSY II of the Helmholtz-Zentrum Berlin: current status and perspectives. *Eur Phys J Plus* **130**, 141–150.